Ganija, Miftar; Ottaway, David John; Veitch, Peter John; Munch, Jesper
Cryogenic, high power, near diffraction limited, Yb:YAG slab laser
Optics Express, 2013; 21(6):6973-6978

Cryogenic, high power, near diffraction limited, Yb:YAG slab laser

Miftar Ganija,[*] David Ottaway, Peter Veitch and Jesper Munch

School of Chemistry and Physics and IPAS, The University of Adelaide, SA 5005, Australia
[*]miftar.ganija@adelaide.edu.au

Abstract: A cryogenic slab laser that is suitable for scaling to high power, while taking full advantage of the improved thermo-optical and thermo-mechanical properties of Yb:YAG at cryogenic temperatures is described. The laser uses a conduction cooled, end pumped, zigzag slab geometry resulting in a near diffraction limited, robust, power scalable design. The design and the initial characterization of the laser up to 200W are presented.

OCIS codes: (140.3460) Lasers; (140.0140) Lasers and laser optics; (140.3480) Lasers, diode-pumped; (140.5560) Pumping; (140.6810) Thermal effects; (140.3615) Lasers, Ytterbium.

References and links

1. P. A. Schulz and S. R. Henion, "Liquid-nitrogen-cooled Ti:Al_2O_3 laser," IEEE J. Quantum Electron. **27**(4), 1039–1047 (1991).
2. P. Lacovara, H. K. Choi, C. A. Wang, R. L. Aggarwal, and T. Y. Fan, "Room-temperature diode-pumped Yb:YAG laser," Opt. Lett. **16**(14), 1089–1091 (1991).
3. D. C. Brown, "Ultrahigh-average-power diode-pumped Nd:YAG and Yb:YAG Lasers," IEEE J. Quantum Electron. **33**(5), 861–873 (1997).
4. G. A. Slack and D. W. Oliver, "Thermal conductivity of garnets and phonon scattering by rare-earth ions," Phys. Rev. B **4**(2), 592–609 (1971).
5. P. H. Klein and W. J. Croft, J, "Thermal conductivity, diffusivity, and expansion of Y_2O_3, $Y_3Al_5O_{12}$, and LaF_3 in the range 77-300 K," Appl. Phys. (Berl.) **38**, 1603 (1967).
6. R. Wynne, J. L. Daneu, and T. Y. Fan, "Thermal coefficients of the expansion and refractive index in YAG," Appl. Opt. **38**(15), 3282–3284 (1999).
7. T. Y. Fan, D. J. Ripin, R. L. Aggarwal, J. R. Ochoa, B. Chann, M. Tilleman, and J. Spitzberg, "Cryogenic Yb3+ doped solid state lasers," invited paper," IEEE J. Sel. Top. Quantum Electron. **13**(3), 448–459 (2007).
8. T. Shoji, S. Tokita, J. Kawanaka, M. Fujita, and Y. Izawa, "Quantum-defect-limited operation of diode-pumped Yb:YAG laser at low temperature," Jpn. J. Appl. Phys. **43**(No. 4A), L496–L498 (2004).
9. D. J. Ripin, J. R. Ochoa, R. L. Aggarwal, and T. Y. Fan, "165-W cryogenically cooled Yb:YAG laser," Opt. Lett. **29**(18), 2154–2156 (2004).
10. D. C. Brown, J. M. Singley, E. Yager, J. W. Kuper, B. J. Lotito, and L. L. Bennett, "Innovative high-power CW Yb:YAG cryogenic laser," Proc. SPIE **6552**, 65520D, 65520D-9 (2007).
11. D. C. Brown, J. M. Singley, E. Yager, K. Kowalewski, J. Guelzow, and J. W. Kuper, "Kilowatt class high-power CW Yb:YAG cryogenic laser," Proc. SPIE **6952**, 69520K, 69520K-9 (2008).
12. D. J. Ripin, J. Ochoa, R. L.Aggarwal, and T.Y. Fan, "300-W cryogenically cooled Yb:YAG laser," IEEE J. Quantum Electron **41**(10), 1274–1277 (2005).
13. High-Power Laser Handbook, Injeyan, H, and Goodno, G, editors, chap 8, McGraw-Hill, 2011.
14. G. D. Goodno, S. Palese, J. Harkenrider, and H. Injeyan, "Yb:YAG power oscillator with high brightness and linear polarization," Opt. Lett. **26**(21), 1672–1674 (2001).
15. M. Ganija, D. J. Ottaway, P. J. Veitch, and J. Munch, "A cryogenic, end pumped, zigzag slab laser suitable for power scaling," in Proceedings of the International Quantum Electronics Conference and Conference on Lasers and Electro-Optics Pacific Rim 2011, (Optical Society of America, 2011), paper.
16. NIST (National Institute of Standards and Technology) Material Measurement Laboratory, Cryogenic Group. *http://cryogenics.nist.gov/MPropsMAY/Molybdenum/Molybdenum_rev.htm*

1. Introduction

Cryogenic solid-state lasers have been shown to offer significant potential for reaching higher powers with better beam quality and higher efficiency than corresponding lasers operating at room temperature [1–3]. The primary advantages arise from an increase in thermal conductivity, a reduction in thermal expansion and a reduced temperature dependence of the refractive index, dn/dT [4–6]. All three factors contribute to significant reductions in the thermo-optical and thermo-mechanical distortions, which in turn enable a given laser medium

#183267 - $15.00 USD Received 10 Jan 2013; revised 20 Feb 2013; accepted 22 Feb 2013; published 13 Mar 2013

to be operated at higher powers and with improved beam quality. Furthermore, in the case of quasi-three level systems, the collapse of the thermal Boltzmann distributions in the lower-state manifold at low temperatures can significantly improve the efficiency of the laser. Excellent detailed discussions of these advantages together with the development of useful figures of merit for cryogenic laser designs have been published [7].

Previous authors have shown that Yb:YAG is almost ideally suited for use at cryogenic temperatures [8–10]. Among the relevant laser hosts tested, they showed that crystalline YAG has the highest thermal conductivity, the lowest thermal expansion coefficient and the smallest dn/dT. Furthermore, the Yb dopant has a high quantum efficiency, no up-conversion or excited state absorption and it becomes an efficient four level laser material at cryogenic temperatures. However, as the dopant concentration is increased, a corresponding increase in phonon scattering tends to reduce the potential cryogenic advantages of the host crystal [4].

The challenge is thus to select a practical laser architecture that can exploit fully the advantages of operating at cryogenic temperatures without introducing new stress-induced wavefront distortion and birefringence caused by differential thermal contraction as the laser head is cooled from 300 K to 77 K. While successful demonstrations of cryogenic Yb:YAG lasers have reported significant improvements in laser performance, distortion free laser architectures optimized for efficiency and high power scaling have not been demonstrated to date. Thin-disc active mirrors offer a small volume-to-cooling-surface ratio, but they require high doping concentrations and relatively complex layouts for efficient pumping [11]. End-pumped rods produce excellent beam quality at medium power levels [12], but the rod architecture ultimately suffers from limitations in power scaling due to effects such as reduced extraction efficiency, residual thermal focusing and complexity of layout. Most authors concentrate on power and slope efficiency, with little emphasis on achieving excellent beam quality and practicality of design. Here we report on the optimization of the laser architecture to maximize the advantages offered by cryogenics, resulting in a compact, efficient and power scalable design with excellent beam quality.

2. Laser design approach

Our objective was to develop a practical design for scaling to high power and making full use of the advantages offered by cryogenic temperature. As mentioned above, this encouraged the use of low doping. Furthermore we wanted to benefit from the lessons learnt when operating high power lasers at room temperature. For these reasons we choose a laser architecture that uses a low-doping, end pumped, side-cooled, zigzag, Yb:YAG laser slab, that has been demonstrated to be scalable to a power in excess of ten kW at room temperature [13].

We have adapted this architecture for use at cryogenic temperatures, subject to additional design constraints, including a practical, conduction cooled approach, the use of readily machinable metal parts where possible, and the ability to cycle the laser repeatedly The optical layout of the laser is shown in Fig. 1, including the vacuum envelope of the cryostat, the windows though which the pump and laser beam pass, as well as the pump optics. The gain medium chosen is a 1 at. % Yb:YAG zigzag slab, of dimensions 50 x 3 x 2 mm, with undoped YAG end-caps, similar to the design described in [14]. It is held by an all metal clamp, forming the "laser head". The laser head and the lens ducts are mounted on an aluminum annulus, which in turn is bolted to the aluminum cold-plate of the cryostat. The gain medium is pumped from both ends using the optical system shown in Fig. 2, where the outputs of fast axis collimated (FAC) laser diode stacks are focused through the cryostat windows into uncoated B270 lens duct using cylindrical telescopes. The light is guided through the lens ducts using total internal reflection (TIR), reflected from the angled end faces of the slab and then confined within the slab by TIR. A simulation using numerical ray-tracing indicated that this scheme provides efficient, uniform pumping of the gain medium with less than 3% loss, if using antireflection coated slabs and lens ducts.

#183267 - $15.00 USD Received 10 Jan 2013; revised 20 Feb 2013; accepted 22 Feb 2013; published 13 Mar 2013

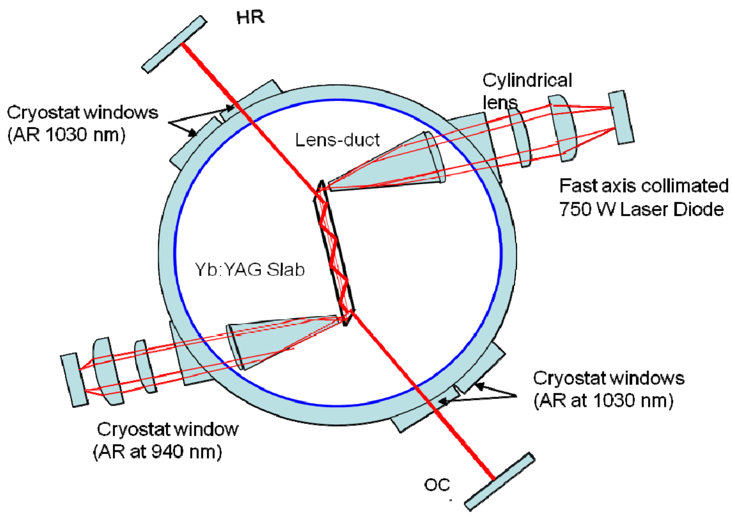

Fig. 1. Schematic of the optical layout of the laser in the cryostat, indicating the anti-reflection coated windows, the external pump laser cylindrical optics telescopes and the high reflectivity (HR) and outcoupler (OC) of the laser resonator

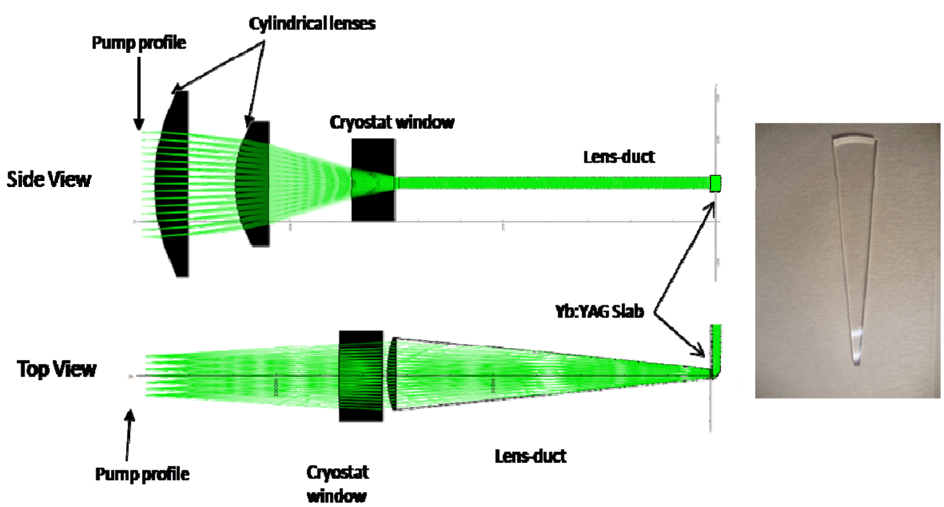

Fig. 2. Schematic of the optimized pump beam configuration, showing top and side views how the lens ducts deposit the pump light into the slab via the AR coated side.

The doped section of the slab is conduction-cooled through the TIR surfaces, which are coated with SiO_2 to prevent disruption of the TIR. End pumping a lightly doped slab and double-sided cooling minimizes the temperature increase in the middle of the gain medium allowing the benefits of cryogenic cooling to be maintained at higher pump powers. Numerical modeling showed that this almost uniform pumping and cooling of the gain medium should result in a one dimensional thermal gradient that is perpendicular to the cooled faces. The effect of the remaining thermal lensing is reduced by the zigzag path of the laser mode, and subsequent power scaling can be done by increasing the height of the TIR surface, without altering thermal properties [13].

3. Cryogenic laser head design

A key design issue for the laser head was to minimize applied stress that could lead to wave-front distortion and induced birefringence [15], while retaining a practical design. We thus

#183267 - $15.00 USD   Received 10 Jan 2013; revised 20 Feb 2013; accepted 22 Feb 2013; published 13 Mar 2013

required that the gain medium could be cooled to cryogenic temperatures without suffering mechanical stress, that it could then be pumped and lase at high power while experiencing minimal additional thermal stress and finally that it could stand repeated cryogenic cycling by ensuring that none of the materials in the laser head exceed their elastic yield point during a cryogenic cycle. To satisfy these requirements, we have developed a composite Yb:YAG-indium-molybdenum-aluminum laser head as shown in Fig. 3.

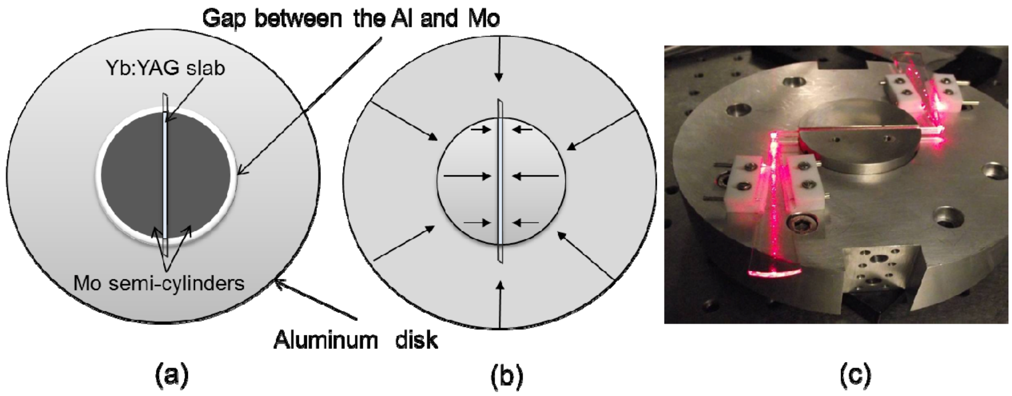

Fig. 3. Schematic of the laser head showing (a) gap between the aluminium annulus and the molybdenum semi-cylinders, (b) the differential thermal contraction of the annulus onto the molybdenum clamping the gain medium and (c) photo of the laser head assembly.

The doped part of the laser slab is clamped between molybdenum semi-cylinders, with the un-doped ends extending beyond the Mo clamp and this clamp extending below the Al annulus to provide optical access to the slab, as shown in Fig. 3(c). A layer of indium, nominal thickness 125 µm, ensures good thermal contact between the slab and molybdenum. At room temperature, there is a small (~50 µm) gap between the molybdenum cylinder and the aluminum annular heat sink, which in turn is bolted to the cold plate of the cryostat. As the laser head is cooled the aluminum annulus contracts differentially onto the molybdenum, thereby firmly clamping it and greatly reducing the thermal resistance between the slab and the cryostat. While we considered other materials such as undoped YAG and sapphire [10] for the material in contact with the slab, we finally chose molybdenum because of the close match between the integrated coefficient of thermal expansion of Mo [16] and YAG [6] over the temperature range considered. Mo also has high thermal conductivity at 77 K, and is readily machinable, resulting in a practical design. The gap between the Al and Mo was optimized to achieve excellent contact without excess stress at 77 K. Finite element analysis showed that the internal stress in the materials used did not exceed the yield points, and this was confirmed by repeated (~100 x) cryogenic cycling of the laser head without deformation.

4. Results and discussion

The performance of the cryogenic design was investigated and optimized using the wave-front distortions caused by cryogenic cooling of the unpumped laser head as the diagnostics. This was measured interferometrically using both a 'straight through' object beam which propagated along the long axis of the slab without TIR, and the zigzag object beam shown in the Fig. 1. The former was used for detailed investigation and minimization of the thermo-mechanical distortions due to cooling and clamping, but since it required the use of the pump windows for access, it could not be used while lasing. Initial results showed significant wavefront distortion and induced birefringence, but as the laser head was optimized as described above, first the birefringence and then the remaining distortions gradually disappeared. Figure 4 shows the final results. Figures 4(a)-4(b) are for the straight through path, with Fig. 4(a) showing the 'zero fringe' and Fig. 4(b) the same scene but with finite fringes to document the interference contrast. Figure 4(c) is equivalent to Fig. 4(a), but using

#183267 - $15.00 USD Received 10 Jan 2013; revised 20 Feb 2013; accepted 22 Feb 2013; published 13 Mar 2013

the zigzag path. This shows that negligible stress is applied to the gain medium by the cooling alone.

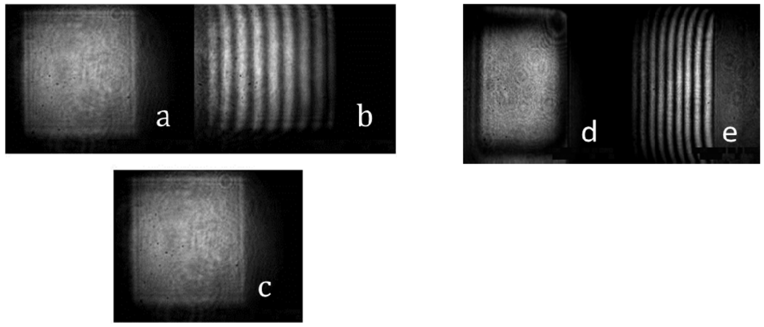

Fig. 4. Interferograms of unpumped gain medium at 77 K: (a) zero-fringe and (b) carrier-fringe, recorded using a 'straight through' probe beam; (c) zero-fringe interferogram recorded using the zigzag probe beam. Figs (d and e) show corresponding interferograms when lasing, at 115W,(pump 208 W)

The gain medium was the fitted with a simple external resonator as shown in Fig. 1. It consisted of a flat highly reflecting (HR) mirror and a 2 m radius-of-curvature, 75% reflectivity, out-coupler (OC), separated by about 50 cm. Interferograms in the zigzag configuration for the cooled laser head, when lasing at 115W, are shown in Figs. 4(d) and 4(e), clearly showing no indication of optical distortions and raising expectations for excellent beam quality. In separate early experiments we used a rotatable crystal polarizer to observe a purely horizontal, linearly polarized output with no evidence of birefringence when lasing at 45W. The output powers observed for two different assemblies of the laser head and the measured beam qualities are shown in Fig. 5. The output power changed by less than 1% during a 15 minute observation, when lasing at 115W. Both sets of data display the same threshold and have a slope efficiency of 64%. Note that the lens ducts were not AR-coated for

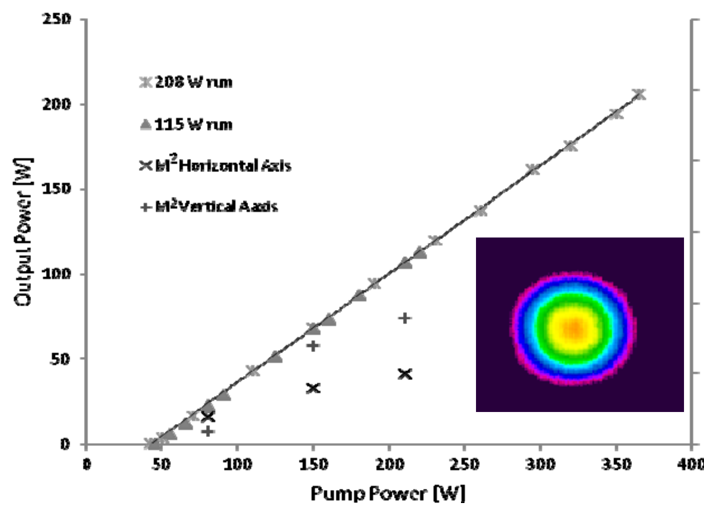

Fig. 5. Output power and M^2 value for both axis of the cryogenically cooled end pumped zigzag slab as a function of incident diode pump power. The insert illustrates the TEM_{00} beam, profile, which was verified by quantitative measurements.

the pump light and so reflected about 9% of the incident power. At a laser output power of 208W, the temperature of the end of the molybdenum clamp, within 2mm of the laser slab, was measured to be 90 K. The wavelength of the output was 1029.6 nm. The beam quality of

#183267 - $15.00 USD Received 10 Jan 2013; revised 20 Feb 2013; accepted 22 Feb 2013; published 13 Mar 2013

the output (M^2) was determined by measuring the variation in beam spot size along the longitudinal axis (z) as the beam was focused through the waist. A Gaussian beam profile was fitted to the results as shown in Fig. 6 and M^2 determined from the fit. The near unity M^2 results obtained are plotted in Fig. 5.

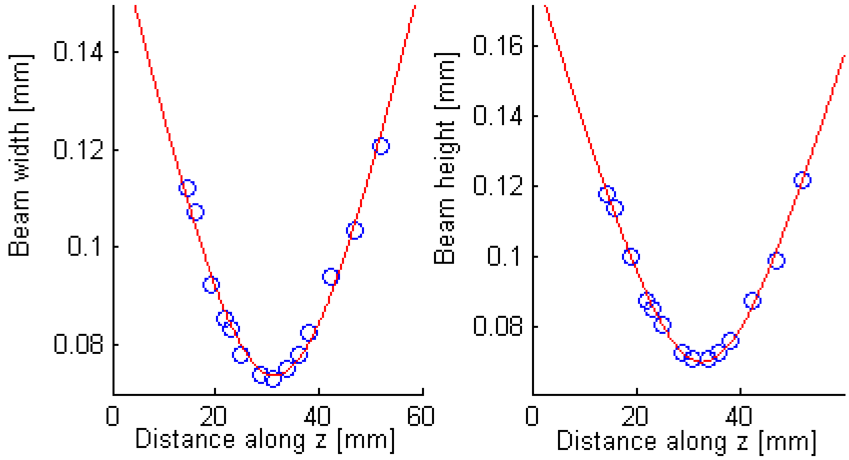

Fig. 6. Gaussian fitting and laser beam profile at 115 W. M^2 of less than 1.1 in vertical direction (non-zigzag) and less than 1.05 in horizontal (zigzag) direction (see Fig. 1)

We were unable to measure the precise beam quality during the final test at 208W due to an untimely and catastrophic electrical failure of a pump diode power supply. However, the, interferograms obtained for this case before the failure looked promising and consistent with earlier non lasing interferometric results which showed no measureable distortions when pumping with up to 400W. By comparison, a slab of the same nominal transverse dimensions, but operating at room temperature, and using a compensated resonator, was reported to have a beam quality approaching 1.7 in the non-zigzag direction when lasing at 250W, and by interpolating the published data we estimated it to be about 1.4 at 115W [14]. Our cryogenic design has thus already demonstrated a significant improvement.

5. Conclusion

We have described what we believe is the first power scalable Yb:YAG laser that can be cooled to cryogenic temperatures to exploit the improvement in thermo-mechanical and optical properties of YAG without introducing wavefront distortions. It produced up to 208W in a TEM_{00} beam. There was no measured degradation in the gain medium and no apparent decrease in slope efficiency. We measured the beam quality accurately to be below 1.1 for powers up to 115W. Since the power scaling demonstrated in [13] was achieved by increasing the area of the cooled surfaces of the slab, and area being the critical parameter for cryogenic cooling, we suggest that by appropriately scaling our design, significantly higher powers should be attainable, ultimately limited by the practicality of the cryostat required.

Acknowledgments

The authors gratefully acknowledge support from the Australian Research Council, the Northrop Grumman Corporation and essential, excellent support from the Physics Workshop at the University of Adelaide.